JOURNAL OF VIROLOGY, Dec. 1997, p. 9770–9777 Vol. 71, No. 12
0022-538X/97/$04.00+0

Allele-Specific Adaptation of Poliovirus VP1 B-C Loop Variants to Mutant Cell Receptors

SA LIAO AND VINCENT RACANIELLO*

Department of Microbiology, Columbia University College of Physicians & Surgeons, New York, New York 10032

Received 12 June 1997/Accepted 7 September 1997

Previous work has shown that three different mutations in domain 1 of the poliovirus receptor (Pvr), two in the predicted C′-C″ ridge and one in the D-E loop, abolish binding of the P1/Mahoney strain. All three receptor defects could be suppressed by a mutation in the VP1 B-C loop of the viral capsid that was present in all 16 P1/Mahoney isolates adapted to the mutant receptors. To identify allele-specific mutations that enable poliovirus to utilize mutant receptors, and to understand the role of the VP1 B-C loop in adaptation, we selected mutant receptor-adapted viruses derived from two P1/Mahoney variants, one which lacks the VP1 B-C loop and one in which the VP1 B-C loop is replaced with the corresponding sequence from the P2/Lansing strain. Six adapted viral isolates were obtained after passage on mutant receptor-expressing cell lines. Sequence analysis revealed that each virus contained three to five mutations, and a total of 18 amino acid changes at 17 capsid residues were identified. Site-directed mutagenesis was used to evaluate the role of these mutations in adaptation to mutant Pvr. The results demonstrate that mutations in the viral canyon floor and rim are allele specific and compensate only for receptor defects in the C′-C″ ridge of Pvr, suggesting that these sites interact in the virus-receptor complex. Furthermore, mutations in the VP1 E-F loop suppressed Pvr D-E loop defects, implying that the Pvr D-E loop contacts the VP1 E-F loop. Most of the other mutations mapped to interior capsid residues, some interacting with the fivefold- or threefold-related protomers. These mutations may regulate receptor interaction by controlling the structural flexibility of the viral capsid. In viruses lacking the VP1 B-C loop, single mutations were not sufficient to confer the adapted phenotype, in contrast to the 414 virus, which contains the B-C loop. Although the VP1 B-C loop appeared to be dispensable for adaptation, it may have provided a selective advantage in adaptation of P1/Mahoney to mutant Pvr.

To initiate infection of cells, viruses must first attach to a cell surface receptor and deliver their nucleic acid to the correct cellular compartment. In some cases the cell receptor is simply a "hook" which facilitates uptake of the virus into the cell, where conformational changes are triggered by low pH or by the action of proteinases. In other cases the interaction of the virus with a cell receptor initiates conformational changes that prime the capsid for uncoating. Poliovirus appears to fall into the latter category. These small, nonenveloped RNA viruses initiate infection by binding to the poliovirus receptor (Pvr), a member of the immunoglobulin superfamily (12). The study of the interaction of poliovirus with Pvr is expected to provide a detailed picture of virus-receptor interaction and how it leads to release of the viral RNA genome into the cell.

The poliovirus capsid is composed of 60 protomers, each containing a single copy of the four capsid proteins, VP1, VP2, VP3, and VP4. Characteristic features of the virion surface include a prominent peak at the fivefold axis of symmetry, a smaller protrusion at the threefold axis of symmetry, a deep surface depression ("canyon") surrounding the fivefold axis of symmetry, and a hydrocarbon-binding pocket underneath the canyon floor (8). The study of soluble receptor-resistant (*srr*) poliovirus mutants demonstrates that capsid residues involved in receptor interaction are located in a region of the canyon which forms part of the protomer interface and in the interior of the virion (2).

The isolation of poliovirus variants adapted to mutant Pvr has provided additional information about capsid residues that control receptor recognition (1). Domain 1 appears to contain the binding site for poliovirus, probably within a 30-amino-acid sequence composed of β-strands C′, C″, and D (see Fig. 1) (reviewed in reference 19). Each of three different mutations within this region block binding of poliovirus type 1 (13). P1/Mahoney variants that can utilize the defective receptors were selected on mutant receptor-expressing mouse L cells, and three mutations in the viral capsid were identified: one on the rim of the canyon, a second near the hydrocarbon-binding pocket, and a third in the VP1 B-C loop, a highly exposed loop at the fivefold axis of symmetry (1).

Mutations in the VP1 B-C loop (P1095S/T; see Table 1, footnote *a*, for an explanation of the nomenclature) were found in each adapted virus, either alone or in combination with a change at one of the other two sites (1). When introduced into wild-type virus, P1095S/T enabled replication on all three mutant receptor-expressing cell lines and is therefore not allele specific. Mutant V1160I, near the hydrocarbon-binding pocket, also did not display allele specificity. However, H2142Y, located on the rim of the canyon, effectively suppressed only two mutations in the C′-C″ strand of Pvr.

We wanted to isolate additional allele-specific suppressor mutations that would reveal residues of the capsid and Pvr that interact. Because the suppressor mutation within the VP1 B-C loop was found in all 16 adapted viruses previously isolated, it seemed likely that it would predominate in any mutant screen using wild-type virus, precluding the identification of new allele-specific suppressors. To circumvent this difficulty, two variants of P1/Mahoney were used to derive mutant receptor-adapted viruses. One virus, Δ9, lacks the VP1 B-C loop (4); in the other variant, 414, the VP1 B-C loop has been replaced

* Corresponding author. Mailing address: Department of Microbiology, Columbia University College of Physicians & Surgeons, 701 W. 168th St., New York, NY 10032. Phone: 212-305-5707. Fax: 212-305-5106. E-mail: vrr1@columbia.edu.

with the corresponding sequence from the P2/Lansing strain (17). Crystallographic analysis of this recombinant virus revealed that the conformation of the VP1 B-C loop of P2/Lansing differs from that of P1/Mahoney (24).

Two Δ9 variants adapted to g cells, one Δ9 variant adapted to i cells, two variants of the 414 virus adapted to g cells, and one variant of 414 adapted to i cells were isolated, demonstrating that the VP1 B-C loop is not required for adaptation to mutant Pvr. Nucleotide sequence analysis of the capsid protein coding region revealed a total of 18 mutations at 17 positions, and each variant harbored 3 to 5 different mutations. Fourteen mutations were introduced singly or in combination into the Δ9 or 414 viral background, and their growth in cells expressing wild-type or mutant Pvr was analyzed. Three mutations in the canyon, H2142Y, D3181N, and S3183R, and three mutations in the VP1 E-F loop, V1160I, W1170R, and T1177S, were able to confer allele-specific adaptation either alone or in combination with one other mutation. These results confirm and extend the hypothesis that Pvr contacts the viral canyon floor and rim and that residues at the protomer interface (VP1 E-F loop) may regulate receptor recognition. Other mutations in adapted viruses were identified in the interior of the virion, and some interact with fivefold- and threefold-related protomers. Although these mutations are in structurally interesting locations, their roles in adaptation to mutant Pvr are not known.

TABLE 1. Mutagenic primers used to generate capsid mutations

Amino acid change[a]	Location (nt) in P1/Mahoney[b]
G4021S	794–820
K4043R	857–883
M4067I	930–956
H2142Y	1382–1328
T2250A	1685–1711
D3181N	2294–2320
S3183R	2300–2326
T1036A	2575–2601
K1103R	2774–2800
V1160I	2945–2971
E1168G	2969–2995
W1170R	2975–3001
T1177S	2996–3022

[a] The first letter is the wild-type amino acid, the first digit identifies the capsid protein, the next three digits identify the amino acid residue, and the final letter is the substituted amino acid.

[b] Nucleotides numbered as in reference 21.

MATERIALS AND METHODS

Cells and viruses. HeLa S3 cells were grown in suspension cultures in Joklik minimal essential medium containing 5% bovine calf serum and 10 μg of gentamycin per ml. For growth in monolayers, HeLa cells were plated in Dulbecco's modified Eagle medium (DMEM) containing 10% bovine calf serum, 100 U of penicillin per ml, and 100 μg of streptomycin (GIBCO) per ml. Stable L-cell transformants expressing wild-type (20B-21) or mutated (d31-3, g28-11, and i212-12) Pvr cDNAs (13) were maintained in DMEM containing 10% bovine calf serum, 100 U of penicillin per ml, 100 μg of streptomycin per ml, and 400 μg of geneticin sulfate (GIBCO) per ml for neomycin resistance. d, g, and i cells express Pvr containing a substitution of Q for F at residue 58, an insertion of VDF between residues 59 and 60, or a replacement of LG with PETN between residues 74 and 75, respectively. Pvr surface levels were periodically determined by fluorescence-activated cell sorting to ensure that they resembled previously determined values (13).

Poliovirus serotype 1 Mahoney was derived by transfecting HeLa cell monolayers with viral RNA produced by in vitro transcription from cloned genomic cDNA (20). P1/Mahoney variants Δ9 and 414 were generous gifts of M. Girard and E. Wimmer, respectively. The generation of poliovirus mutants is described in detail below. To prepare viral stocks, plaque-purified virus was inoculated into HeLa cell monolayers or cells expressing mutant Pvr. Viral titers were determined by plaque assay on HeLa cell monolayers as described previously (21) or on monolayers of cells expressing mutant Pvr.

Selection of Δ9 and 414 mutants adapted to d, g, or i receptors. Initially, four plaque-purified stocks containing 4×10^7 to 1×10^8 PFU of Δ9 or 414 were incubated with monolayers of d, g, or i cells for 45 min at 37°C. After absorption, the monolayers were overlaid with agar and incubated at 37°C for 3 days. No plaques were observed. Subsequently, the same amount of viral inoculum was used for infection, and after absorption, monolayers were overlaid with liquid media and incubated at 37°C for 2 days. Virus was harvested and 100 μl of the stock was used to reinfect fresh monolayers of cells expressing mutant Pvr. This process was repeated until cytopathic effect (CPE) was observed. Usually one to three passages were required before CPE developed. Viruses were then subjected to three rounds of plaque purification. Finally, stocks of adapted viruses were prepared in the cell lines in which selection was carried out.

Identification of mutations in the Δ9 and 414 adapted viruses. To amplify viral mutants, confluent 15-cm-diameter plates of g and i cells were inoculated with adapted viruses. After 2 days at 37°C, virus was harvested as described above and pelleted by centrifugation through a 30% sucrose cushion at 38,000 rpm and 10°C in an SW41 rotor. Pellets were resuspended in NTE buffer (10 mM NaCl, 50 mM Tris-HCl [pH 8.0], 10 mM EDTA) containing 0.5% sodium dodecyl sulfate, and viral RNA was extracted (9) and used as a template for first-strand cDNA synthesis. cDNA synthesis was carried out for 30 min at 37°C in a 50-μl mixture containing 1× first-strand buffer (GIBCO), 10 mM dithiothreitol, 1 mM (each) deoxynucleoside triphosphates, 50 U of RNasin (Promega), 400 U of Superscript II reverse transcriptase (RT) (GIBCO), and 100 ng of oligo(dT) (GIBCO). The first-strand cDNA was used as a template for PCR with Vent DNA polymerase (New England Biolabs) according to the manufacturer's recommendations. To amplify cDNA encoding the entire capsid, the following two primers were used: a sense primer that hybridizes to nucleotides (nt) 487 to 506 and an antisense primer that hybridizes to nt 3410 to 3427. The 3.1-kb PCR product was treated with T4 polynucleotide kinase (New England Biolabs) and cloned into the *Eco*RV site in pBR322.

The nucleotide sequence of the entire capsid cDNA was determined by the dideoxy method (22) to identify mutations. To confirm the presence of a mutation in the viral RNA, RNA was extracted from virus as described above and its sequence was determined with avian myeloblastosis virus RT (Boehringer Mannheim) as described previously (9). Due to technical difficulties in sequencing, some mutations could not be confirmed by RNA sequencing. For these mutations, viral RNA was used as a template for three independent RT-PCR reactions, with oligo(dT) as the primer in RT reactions and different combinations of primers in PCRs to amplify fragments containing VP1, VP2, VP3, or VP4. The primer usage was the same as in the site-directed mutagenesis as described below, with the exception that the antisense primers used to amplify VP2 annealed to nt 1955 to 1972 or nt 2132 to 2149. The RT-PCR products, approximately 1 kb in length, were sequenced directly by Ampli-*Taq* cycle sequencing (Perkin-Elmer) according to the manufacturer's protocol. If a mutation was present in all three independent RT-PCR fragments, its presence in the viral RNA was considered confirmed.

Site-directed mutagenesis. Single mutations were introduced by recombinant PCR (6) by using two mutagenic primers and two nonmutagenic flanking primers. A *Sac*II site was created at residue 12 in $2A^{pro}$ protease without changing the amino acid sequence. Nonmutagenic primers included a sense primer that hybridizes with nt 2947 to 2967 and an antisense primer that hybridizes with nt 5592 to 5613. Both mutagenic primers hybridized with nt 3411 to 3430. The introduction of a *Sac*II site in $2A^{pro}$ did not affect viral growth, as determined by one-step growth analysis (10). PT7MSacIIΔA/ΔS, a plasmid containing full-length P1/Mahoney cDNA with the *Sac*II mutation, a T7 promoter for production of the viral RNA transcripts, and a ~4-kb pBR322 *Bam*HI-*Eco*RI fragment lacking the *Aat*II and *Ssp*I sites, was used for mutagenesis. The VP1 B-C loop deletion (Δ9) or substitution with sequences from P2/Lansing (414) was introduced into this plasmid as follows. The VP1 coding sequence was amplified from Δ9 and 414 cDNAs (generous gifts of M. Girard and E. Wimmer, respectively) in PCRs using a sense primer annealed to nt 2462 to 2482 and an antisense primer annealed to nt 3396 to 3428. The 1-kb product was digested with *Nhe*I and *Sna*BI (New England Biolabs) and cloned into PT7MSacIIΔA/ΔS. Nucleotide sequence analysis confirmed that the resulting cDNAs contained only the intended changes. The two plasmids, PT7Δ9 and PT7414, were used as vectors for subsequent cloning or as templates for PCRs.

To introduce mutations into capsid cDNA, cDNA of the appropriate capsid protein was amplified by recombinant PCR, digested, and ligated into PT7Δ9 or PT7414. The two nonmutagenic flanking primers annealed with the following sites: VP4, nt 332 to 349 and 1205 to 1222; VP2, nt 931 to 955 and 1769 to 1786; VP3, nt 1676 to 1693 and 2486 to 2503; and VP1, nt 2462 to 2482 and 3396 to 3428. Restriction enzyme cleavage sites used to clone the PCR products into PT7Δ9 or PT7414 were *Age*I and *Aat*II for VP4, *Aat*II and *Ssp*I for VP2, *Ssp*I and *Nhe*I for VP3, and *Nhe*I and *Sac*II for VP1. The sense and antisense mutagenic primers used are listed in Table 1. Nucleotide sequence analysis was used to confirm that the intended mutation was present.

This strategy was used to introduce single amino acid changes at 13 different positions in Δ9 or 414 cDNA. For every mutation that was introduced, each PCR was performed in duplicate and two independent viruses were studied, to minimize the risk that a phenotype was due to a mutation introduced by PCR.

The mutagenized viral cDNA was transcribed in vitro with T7 RNA polymer-

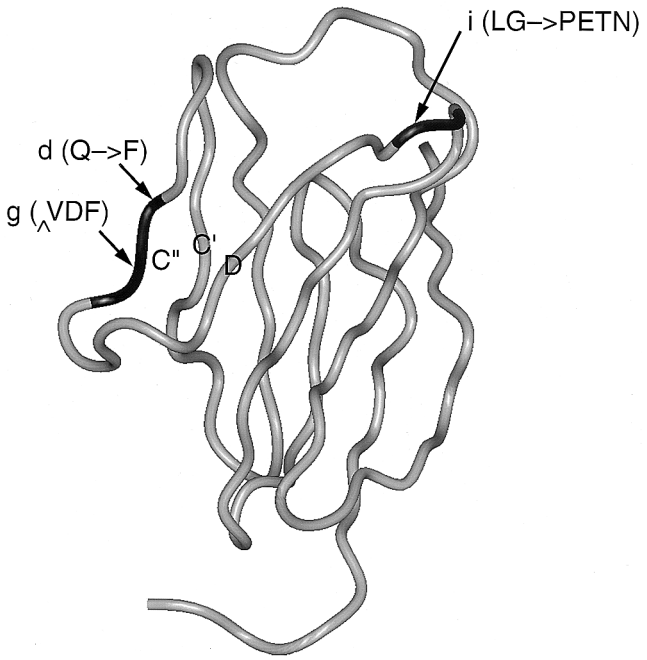

FIG. 1. Model of Pvr domain 1 showing the d, g, and i mutations. The structure of domain 1 was predicted as described previously (13). The C′, C″, and D β-strands are labeled. The amino acid changes of the d, g, and i mutations are shown, and the corresponding regions of Pvr are highlighted in black.

ase, viral RNA products were transfected into HeLa cells (1), and virus was harvested for plaque assay or further amplified for binding assays.

Computer graphics. The atomic coordinates for P1/Mahoney and v510 (the latter is the equivalent of 414 but was isolated by others [24]) were provided by James M. Hogle. The capsid structure was visualized on a Silicon Graphics Indigo 2 Impact by using Insight II, version 95 (Biosym Technologies Inc., San Diego, Calif.).

RESULTS

Selection of Δ9 and 414 viral mutants adapted to cells expressing mutant Pvr. To identify allele-specific mutations in the poliovirus capsid that compensate for receptor defects, we selected adapted viruses by using two P1/Mahoney VP1 B-C loop variants. One virus, Δ9, lacks the VP1 B-C loop (4), and in the other variant, 414, the VP1 B-C loop has been replaced by the corresponding sequence from the P2/Lansing strain (17). Three stable L-cell lines called d, g, and i, which express Pvr mutants that fail to bind P1/Mahoney (Fig. 1) (13), were used.

To select for adapted mutants, viruses were passaged on d, g, and i cell monolayers until CPE was observed. Each mutant was derived from an independent virus stock and was subjected to three rounds of plaque purification on the cell lines from which it was isolated. Viral titers were then determined by plaque assay on the different cell lines. Stocks of Δ9 and 414 which typically yielded 7×10^8 to 8×10^8 PFU/ml on wild-type Pvr-expressing cells failed to form plaques on mutant Pvr-expressing cells (Table 2). After passage on d, g, or i cells, two Δ9 g-adapted viruses, one Δ9 i-adapted virus, two 414 g-adapted viruses, and one 414 i-adapted virus were obtained (Table 2). For unknown reasons, passage of both viruses on d cells failed to yield d-adapted viruses, although 414 variants adapted to g cells were also able to grow on d cells. All adapted viruses retained the ability to grow on 20B cells, which express wild-type Pvr (Table 2). The two Δ9 variants selected on g cells were able to grow only on g cells, while the Δ9 virus selected on i cells was able to grow on both g and i cells. The 414-2/g and 414-3/g viruses were able to grow on d and g cells, and the 414-3/i virus was able to grow on g and i cells.

TABLE 2. Growth of Δ9, 414, and adapted viruses on d, g, i, and 20B cells[a]

Virus	Selecting cell type	Passage no.	Titer (PFU/ml)[b]			
			d cells	g cells	i cells	20B cells
Δ9-1/g[c]	g	3	<10	3.9×10^5	<10	5.0×10^6
Δ9-3/g	g	3	<10	4.5×10^6	<10	8.9×10^5
Δ9-1/i	i	3	<100	4.6×10^6	1.6×10^6	2.5×10^7
414-2/g	g	1	8.9×10^6	3.0×10^7	<10	1.0×10^8
414-3/g	g	1	2.1×10^5	5.7×10^7	<10	7.5×10^7
414-3/i	i	2	<10	3.7×10^4	6.5×10^5	4.6×10^7
Δ9	NA[d]	NA	<10	<10	<10	8.5×10^8
414	NA	NA	<10	<10	<10	7.3×10^8

[a] d, g, i, and 20B cells are L cells expressing d, g, i, and wild-type Pvr, respectively.
[b] Determined by plaque assay on d, g, i, and 20B cells. Δ9 and 414 titers were the averages of the four stocks.
[c] Δ9-1/g stands for g-adapted viruses derived from stock 1 of the four Δ9 stocks. Similar terminology was used for 414 adapted viruses.
[d] NA, not applicable.

Identification of mutations in adapted viruses and their locations on the capsid structure. To identify the mutation(s) in adapted viruses, cDNAs encoding the capsid regions were molecularly cloned and their nucleotide sequences were determined. The presence of the identified mutations in viral RNA was confirmed by sequencing specific regions of the viral RNA or by sequencing at least three independent RT-PCR fragments derived from viral RNA. Eighteen mutations at 17 residues were identified among the six viral isolates (Table 3). Each virus contained three to five different mutations, and independent clones with the same growth phenotype had different combinations of mutations. For example, Δ9-1/g and Δ9-3/g grow on 20B and g cells but contain different mutations.

Examination of the three-dimensional structure of poliovirus showed that D3181 and S3183 are located in the canyon floor at the interface between protomers, and H2142 maps to the canyon rim (Fig. 2). V1160, E1168, W1170, and T1177 are part of the VP1 E-F loop, which lies in the interface between protomers. K1103 is located in the VP1 B-C loop, and D1247 maps to the VP1 H-I loop. Both the B-C and H-I loops of VP1 are highly exposed on the viral surface at the fivefold axis of symmetry. R3071, located in the VP3 B strand, is also exposed on the virion surface. All other mutations occur on interior capsid residues. Among them, K4043 is near the fivefold-related protomer (Fig. 2). Four other residues, including T1036, T2250, I3155, and M4067, lie near the threefold-related protomer. T1036 contributes to the formation of the seven-

TABLE 3. Capsid mutations in Δ9 and 414 adapted viruses

Virus	Mutation[a]
Δ9-1/g	K4043R, R3071Q, S3183R, D1247G
Δ9-3/g	V2124I, H2142Y, D3181N, I3155V, T1036A
Δ9-1/i	V1160I, W1170R, T1177S
414-2/g	G4021S, M4067T, T2250A, S3183R
414-3/g	M4067I,[b] H2142Y, D3181N
414-3/i	G4021S, M4067I, K1103R, E1168G

[a] Nomenclature as in Table 1. Underlining indicates mutations that were identified in more than one isolate.
[b] M4067I is present in the parent 414 virus.

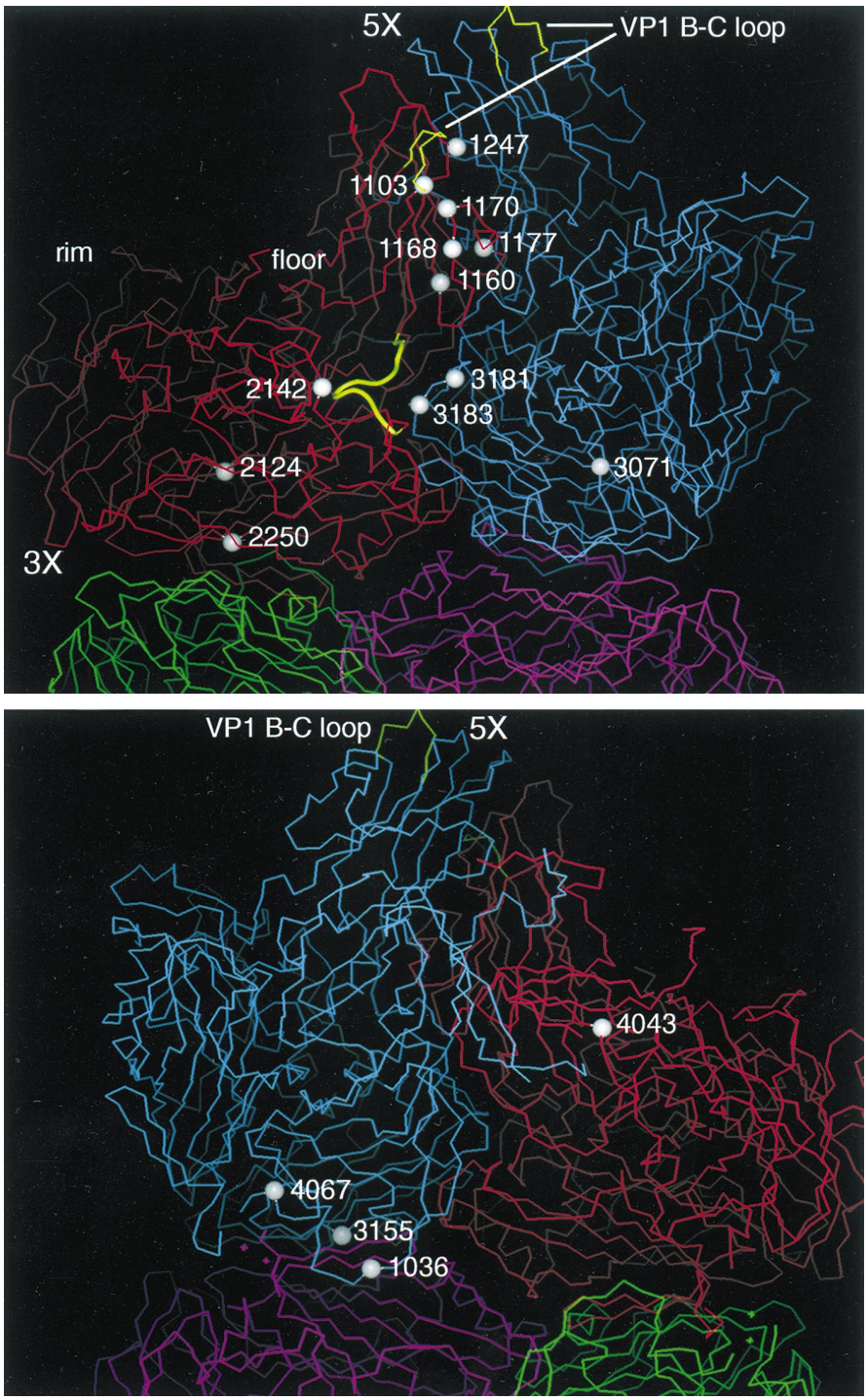

FIG. 2. Location in the poliovirus capsid of 16 mutations identified in adapted viruses. (Top) α-Carbon trace of four protomers viewed from the outside of the virion (60 protomers form an entire capsid). Individual protomers are colored blue, red, green, and magenta. The blue and red protomers are fivefold (5×)-related protomers; the magenta and green protomers are the threefold (3×)-related protomers for the blue and red protomers. The VP1 B-C loop at the fivefold axis of the blue and red protomers is colored yellow. The yellow tube is the VP1 G-H loop, in which the majority of *srr* mutations are located. The yellow tube is part of the canyon floor, which encircles the fivefold axis; the canyon rim is also labeled. Adapting mutations are shown as white spheres, and the residue numbers are indicated. (Bottom) The four protomers from the top panel rotated ~180° and viewed from the inside of the virion, showing the locations of four interior mutations. The color coding and labeling are the same as for the top panel.

stranded β-sheet, which is an essential interpentamer structure (Fig. 2).

Identification of adapting mutations in the viral capsid. To identify the role of individual mutations in adaptation to mutant Pvr, site-directed mutagenesis was performed to introduce mutations into the Δ9 or 414 viral background. Fourteen mutations were introduced into the parental viruses at 13 different positions.

TABLE 4. Growth of site-directed mutant viruses containing mutations identified in Δ9-1/g and Δ9-3/g viruses on d, g, i, and 20B cells

Virus	Titer (PFU/ml)[a]			
	d cells	g cells	i cells	20B cells
Δ9-1/g	<10	3.9×10^5	<10	5.0×10^6
Δ9-S3183R	<10	<10	<10	8.1×10^6
Δ9-K4043R	<10	<10	<10	6.9×10^7
Δ9-S3183R + K4043R	<10	3.0×10^7	3.9×10^6	2.3×10^8
Δ9-3/g	<10	4.5×10^6	<10	8.9×10^5
Δ9-H2142Y	<10	<10	<10	4.1×10^7
Δ9-D3181N	<10	<10	<10	1.2×10^7
Δ9-T1036A	<10	<10	<10	1.3×10^8
Δ9-H2142Y + D3181N	<10	8.3×10^7	<10	7.9×10^6

[a] Titers of site-directed mutants were determined for two independent isolates generated from independent PCR mutagenesis. In all cases the titers of the two isolates differed by less than 1 $\log_{10}$ PFU. The titer of only one isolate is shown in Tables 4 through 8.

Two mutations identified in the Δ9-1/g virus, S3183R and K4043R, were introduced singly into Δ9. Single mutants Δ9-S3183R and Δ9-K4043R were unable to grow on any of the mutant receptor-expressing cell lines (Table 4). However, double mutant Δ9-S3183R + K4043R was able to replicate on both g cells and i cells (Table 4). Because Δ9-1/g virus was able to multiply only on g cells, it is likely that one or both of the additional mutations identified in that virus, R3071Q and D1247G (Table 3), suppressed its growth on i cells.

Three mutations identified in the Δ9-3/g virus, H2142Y, D3181N, and T1036A, were introduced into the Δ9 virus. None of the resulting single mutants grew on any of the mutant receptor-expressing cell lines (Table 4). The double mutant Δ9-H2142Y + D3181N was able to grow on g cells, as does the Δ9-3/g virus. The three additional mutations identified in the Δ9-3/g virus (Table 3) are apparently not necessary for adaptation of the Δ9-3/g virus to the g receptor.

The three mutations identified in the Δ9-1/i virus (Table 3) all map to the VP1 E-F loop, which lies in the interface between protomers. Single mutants Δ9-V1160I, Δ9-W1170R, and Δ9-T1177S did not grow on any mutant receptor-expressing cell lines (Table 5). Double mutants harboring any combination of these three mutations were able to replicate on g cells (Table 5). A virus containing all three mutations was able to multiply on both g cells and i cells and therefore had the same phenotype as the Δ9-1/i virus (Table 5).

All adapted viruses derived from 414 contain a mutation of M4067 (Table 3). In 414-3/g and 414-3/i, residue 4067 had one nucleotide change in its codon and was mutated to isoleucine.

TABLE 5. Growth of site-directed viruses containing mutations identified in Δ9-1/i viruses on d, g, i, and 20B cells

Virus	Titer (PFU/ml)			
	d cells	g cells	i cells	20B cells
Δ9-1/i	<10	4.6×10^6	1.6×10^6	2.5×10^7
Δ9-V1160I	<10	<10	<10	2.3×10^8
Δ9-W1170R	<10	5.1×10^2	<10	4.3×10^7
Δ9-T1177S	<10	<10	<10	8.6×10^7
Δ9-V1160I + W1170R	<10	1.5×10^7	<10	2.6×10^7
Δ9-V1160I + T1177S	<10	5.2×10^5	<10	2.8×10^7
Δ9-W1170R + T1177S	<10	1.5×10^7	<10	9.3×10^7
Δ9-V1160I + W1170R + T1177S	<10	6.2×10^6	3.3×10^6	2.6×10^7

TABLE 6. Growth of site-directed viruses containing mutations identified in 414-2/g viruses on d, g, i, and 20B cells

Virus	Titer (PFU/ml)			
	d cells	g cells	i cells	20B cells
414-2/g	8.9×10^6	3.0×10^7	<10	1.0×10^8
414-S3183R	<10	8.0×10^7	<10	3.2×10^7
414-M4067T	<10	<10	<10	1.7×10^8
414-S3183R + M4067T	<10	5.8×10^3	<10	3.1×10^4
414-S3183R + M4067T + G4021S + T2250A[a]	NA	NA	NA	NA

[a] This cDNA construct, after in vitro transcription and transfection into HeLa cells, did not yield infectious virus. NA, not applicable.

In 414-2/g, this codon had two nucleotide changes and residue 4067 was mutated to threonine. Subsequently, M4067I was found to be present in the parent 414 virus. Because the 414 plasmid used for mutagenesis did not contain this mutation (see Materials and Methods), the effect of this change on adaptation was determined. However, introduction of M4067I into 414 resulted in a virus that was unable to grow on any of the mutant receptor-expressing cell lines (Table 7).

The 414-2/g virus, which can grow on d and g cells (Table 2), contains four mutations: S3183R, M4067T, G4021S, and T2250A. Single mutant 414-S3183R was adapted only to the g receptor (Table 6); this mutation is therefore allele specific. 414-M4067T was not adapted to any of the mutant receptor-expressing cell lines (Table 6). Viral RNA of the double mutant 414-S3183R + M4067T repeatedly yielded ~10^4 PFU/ml or less after transfection into HeLa cells, and the titer could not be increased after passage in HeLa cells (10). Despite its low titer, the double mutant was clearly able to replicate on g cells (Table 6). The M4067T mutation therefore has no apparent contribution to adaptation (Table 6), although it appears to impair viral growth when combined with the S3183R mutation. Viral cDNA containing all four mutations was also constructed, but after in vitro transcription and transfection into HeLa cells, no infectious virus was produced. Since 414-2/g contains these four capsid mutations, we hypothesize that a mutation(s) in another part of the viral genome rescued this lethal phenotype.

The 414-3/g virus contains two mutations, H2142Y and D3181N, in addition to the parental mutation M4067I (Table 3). Single mutant 414-H2142Y was adapted only to d cells; this mutation is therefore allele specific (Table 7). Single mutant 414-D3181N was not adapted to any of the mutant receptor-expressing cell lines (Table 7). However, double mutant 414-D3181N + H2142Y was able to grow on both d and g cells (Table 7). Its ability to grow on d cells can be attributed to the mutation H2142Y, and its ability to grow on g cells seems to be

TABLE 7. Growth of site-directed viruses containing mutations identified in 414-3/g viruses on d, g, i, and 20B cells

Virus	Titer (PFU/ml)			
	d cells	g cells	i cells	20B cells
414-3/g	2.1×10^5	5.7×10^6	<10	7.5×10^7
414-D3181N	<10	2.6×10^3	<10	1.1×10^9
414-H2142Y	1.7×10^7	<10	<10	9.7×10^8
414-M4067I	<10	<10	<10	9.7×10^7
414-D3181N + H2142Y	6.0×10^6	3.0×10^7	<10	1.6×10^8
414-D3181N + H2142Y + M4067I	9.0×10^7	3.1×10^6	<10	5.2×10^7

TABLE 8. Growth of site-directed viruses containing mutations identified in 414-3/i viruses on d, g, i, and 20B cells

Virus	Titer (PFU/ml)			
	d cells	g cells	i cells	20B cells
414-3/i	<10	3.7×10^4	6.5×10^5	4.6×10^7
414-E1168G	<10	8.0×10^2	<10	6.1×10^8
414-K1103R + M4067I	<10	<10	<10	7.3×10^8
414-G4021S + M4067I	<10	<10	<10	6.7×10^8
414-E1168G + K1103R + G4021S + M4067I	<10	1.3×10^4	3.3×10^4	1.1×10^7

a combinatorial effect of H2142Y and D3181N. Triple mutant 414-D3181N + H2142Y + M4067I had the same adapted phenotype as the double mutant (Table 7). Therefore, the parental mutation M4067I made no apparent contribution to the adapting phenotype.

The 414-3/i virus contains three mutations besides the parental M4067I: K1103R, E1168G, and G4021S (Table 3). G4021S was also present in 414-2/g. Single mutant 414-E1168G and double mutants 414-K1103R + M4067I and 414-G4021S + M4067I were unable to grow on any of the mutant receptor-expressing cell lines (Table 8). A mutant virus containing all four changes was adapted to g and i cells, the same adapted phenotype as the 414-3/i virus (Table 8).

DISCUSSION

The goal of this work was to identify allele-specific suppressor mutations in the poliovirus capsid that compensate for binding defects of mutant Pvr's. A previous study of poliovirus adaptation to mutant receptors revealed that mutations in the VP1 B-C loop predominate in adapted viruses, and such mutations are not allele specific (1). To circumvent this limitation, two P1/Mahoney VP1 B-C loop variants—Δ9, which lacks the VP1 B-C loop (4), and 414, in which the VP1 B-C loop has been replaced by the corresponding sequence from the P2/Lansing strain (17)—were used to derive mutant receptor-adapted viruses. The results reveal new allele-specific mutations on the poliovirus capsid that confer mutant Pvr adaptation. These mutations do not affect the ability of poliovirus to recognize wild-type Pvr and therefore expand receptor specificity.

d- and g-adapting mutations reveal specific canyon residues that may contact the C′-C″ ridge of Pvr. A comparison of the crystallographic structures of P1/Mahoney and 414 (8, 24) reveals that the Pvr binding sites on each virus, believed to be located in the viral canyon (2), are identical. Therefore, conclusions made in this study with the 414 virus are likely to apply to P1/Mahoney. Based on two observations, it seems likely that canyon residue 2142 (Fig. 2) contacts residue Q58 in the C′-C″ ridge of Pvr (Fig. 1). The mutation H2142Y specifically adapts the 414 virus to the d receptor, which has a point mutation at Pvr residue 58 in the C′-C″ ridge. Furthermore, both H2142 and Y2142 are exposed on the canyon rim in P1/Mahoney and are adjacent to several *srr* mutations (Fig. 2) (2, 23). In the d receptor, the Q58F mutation might disrupt the interaction with H2142, abolishing viral binding. In 414-H2142Y, the tyrosine residue may be involved in strong hydrophobic interactions with the phenylalanine of Pvr, restoring binding.

Addition of a second mutation, D3181N, to 414-H2142Y enables this virus to grow on both d and g cells. D3181 is located on the canyon floor (Fig. 2) and is also close to several *srr* mutations (2). In P1/Mahoney part of the side chain of D3181 is highly exposed on the virus surface and could be involved in direct interaction with the receptor. The new side chain might also point outward and interact with Pvr. These changes alone are insufficient for adaptation because 414-D3181N fails to grow on d, g, or i cells.

Mutant 414-S3183R is specifically adapted to the g receptor. S3183 is partially exposed on the canyon floor (Fig. 2), and a change to G at this position was previously identified as an *srr* mutation (2). Increased binding might be due to the formation of a salt bridge between R3183 and D inserted into the g receptor. Because residue 3183 is located at the protomer interface, a change at this position might also make the virus more susceptible to receptor-induced conformational transitions, compensating for the defect in the g receptor at a post-binding step.

Adaptation to g and i cells requires two mutations in viruses lacking a VP1 B-C loop. The single mutants Δ9-H2142Y and Δ9-S3183R are not adapted to mutant receptors, although the same mutations in a 414 viral background resulted in adaptation to d and g cells, respectively. These results could be explained if the receptor binding site were different in Δ9 virus as a consequence of the deletion of the VP1 B-C loop. However, crystallographic studies of the Δ9 virus reveal that changes in the canyon are minimal (7). Perhaps the lack of a VP1 B-C loop prevents optimal receptor recognition, necessitating two suppressor mutations.

Growth of the Δ9 virus on g cells is enabled by the presence of one of two pairs of mutations: H2142Y plus D3181N and S3183R plus K4043R; the latter combination also permits replication on i cells. An explanation for the lack of allele specificity of S3183R plus K4043R might be that adaptation results in part from conformational changes caused by the K4043R mutation, which alone is insufficient to confer adaptation. Located near the fivefold-related protomer (Fig. 2), K4043 forms both intraprotomer hydrogen bonds with S4042 and D4045 and an interprotomer hydrogen bond with E4014 in the fivefold-related protomer. Residue S4047 is in the same area as its corresponding residue in P3/Sabin and is involved in the resistance to capsid-binding drugs (16). Therefore, changing lysine to arginine may destabilize the pentamer and increase virion flexibility, leading to expanded receptor recognition.

Locations of other residues identified in Δ9 and 414 g-adapted viruses. The three interior mutations identified in Δ9-3/g, V2124I, I3155V, and T1036A, are not essential for growth of Δ9 in g cells. T1036A does not permit growth in g cells, and it was not determined whether the other two mutations individually or all three in combination permit growth. Their presence in structurally interesting locations in the capsid suggests that they may play a role in adaptation. I3155 and T1036 are located near the threefold-related protomer (Fig. 2). T1036, part of the seven-stranded β-sheet which links adjacent pentamers, forms an interpentamer hydrogen bond with T2017 from the threefold-related protomer. I3155 contributes to pentamer stability by forming two interpentamer hydrogen bonds with T2024 and T2022 from the threefold-related protomer. Other residues in this area have been shown to regulate the mouse neurovirulence of P1/Mahoney and the resistance of the P3/Sabin strain to capsid-binding drugs, perhaps by regulating the flexibility of the virion (3, 15). V2124 is within the VP2 E strand (Fig. 2) and forms a hydrogen bond with N2196. It is also close to I2231, which is the site of an *srr* mutation (2), and A2206, whose corresponding residue in P3/Sabin confers resistance to capsid-binding drugs (15). If any of these residues play a role in adaptation, they may do so by modulating the flexibility of the capsid and its ability to recognize mutant receptors.

Three internal mutations were identified in 414-2/g: G4021S, M4067T, and T2250A. The first two are not required for adaptation to g cells. Due to a lack of crystallographic data, G4021 cannot be identified in the capsid structure. M4067 is near the threefold-related protomer, in the same area as T1036 and I3155 (Fig. 2) (see previous paragraph). M4067 is also in the vicinity of I4062, which enables P1/Mahoney to persistently infect a human neuroblastoma cell line and to paralyze mice (3). T2250A was not tested singly in the 414 virus, so it is not known if it is an adapting mutation. T2250 is also located near the threefold-related protomer (Fig. 2) and forms three intraprotomer hydrogen bonds, one with T2068 and two with Q2111. It also forms an interpentamer hydrogen bond with Q3195 from the threefold-related protomer.

Two additional residues identified in the Δ9-1/g virus are R3071 and D1247. The contribution of these mutations to adaptation was not determined, because the two mutations K4043R and S3183R together were sufficient to permit growth of Δ9 on g and i cells. However, the combination of all four mutations in Δ9 prevents replication in i cells. This effect may be due to the presence of R3071Q and/or D1247G. R3071 is in the B strand of VP3 and D1247 is located in the VP1 H-I loop at the fivefold axis of symmetry (Fig. 2), but the significance of mutations at these locations is unknown.

i-adapted viruses identify mutations in the VP1 E-F loop. All three mutations found in Δ9-1/i, V1160I, W1170R, and T1177S, are required for adaptation to i cells, and all of these are located in the VP1 E-F loop (Fig. 2), which is between two fivefold-related protomers. Of the three mutations required for adaptation of 414 to i cells, one mutation, E1168G, is also located in the VP1 E-F loop (Fig. 2). Residues 1160 and 1177 are buried, while residues 1168 and, to a lesser extent, 1170 (since most of the W1170 side chain is buried) are accessible on the virus surface. The fact that both i-adapted viruses contain mutations in the VP1 E-F loop suggests that the region of Pvr containing the i mutation (Fig. 1) might contact the VP1 E-F loop. Interestingly, when mutations restore the ability to interact with i receptors, they invariably recognize g receptors as well. Because the VP1 E-F loop forms part of the interface between protomers, mutations in this loop are likely to have a general influence on the stability of the capsid (1, 2, 5), leading to the absence of allele specificity. Any pairwise combination of these three mutations leads to allele-specific adaptation of Δ9 to g cells. However, V1160, W1170, and T1177 are not likely to be contact sites for the C′-C″ ridge of Pvr because they are distant from other capsid residues that appear to bind the ridge. Perhaps mutations in the VP1 E-F loop produce specific conformational changes at the receptor binding site, leading to allele specificity.

In addition to E1168G, two additional mutations outside of the VP1 E-F loop are required for adaptation of 414 to i cells: one in the interior of the capsid (G4021S, for which no structure is available), and one in the VP1 B-C loop (K1103R). K1103 forms hydrogen bonds with N1094, N1246, and V1244, which may be disrupted by the change to R. These mutations may influence the structure of the neighboring VP1 E-F loop at the protomer interface, which might alter receptor recognition.

The role of the VP1 B-C loop in adaptation to d, g, or i receptors. Because the binding affinities of Δ9 and P1/Mahoney viruses to Pvr do not differ significantly (10), the VP1 B-C loop is unlikely to directly contact the receptor. However, the VP1 B-C loop may play a role in controlling virion conformation, thereby influencing receptor binding. In support of this idea are the findings that (i) all P1/Mahoney mutants adapted to d, g, or i mutant receptors have a change, P1095S/T, in the VP1 B-C loop which alone is sufficient to confer adaptation (1); (ii) the Δ9 virus exhibits small-plaque and heat-labile phenotypes, suggesting that the VP1 B-C loop regulates virion flexibility (4); and (iii) the VP1 B-C loop is a determinant of mouse neurovirulence of the P2/Lansing strain and has been suggested to permit recognition of a mouse receptor (11, 14, 17, 24).

The emergence of the Δ9/g and Δ9/i viruses argues against the possibility that structural flexibility provided by the VP1 B-C loop is essential for adaptation. However, adaptation of the Δ9 virus to g and/or i cells requires at least two mutations at seven different positions, four of which are well conserved among poliovirus serotypes (18). In contrast, single mutations suffice to adapt P1/Mahoney to mutant receptors, and all of these mutations occur at nonconserved residues (18). These observations suggest that the P1/Mahoney VP1 B-C loop provides some selective advantage for adaptation.

In conclusion, the study of the Δ9 and 414 polioviruses adapted to d, g, and i cells reveals residues that may be involved in virus-receptor interaction. The allele-specific interactions suggest that H2142 contacts residue 58 on the Pvr C′-C″ ridge and that D3181 and S3183 are also part of or near the contact site. i-adapting mutations are mostly clustered in the VP1 E-F loop, suggesting that this region contacts the Pvr D-E loop. Residues on the capsid surface may also influence receptor-mediated alterations of the virus structure that are necessary for receptor interaction. Resolution of the crystallographic structure of a poliovirus-Pvr complex will reveal the accuracy of the models predicted by these genetic analyses.

ACKNOWLEDGMENTS

We thank M. Girard and E. Wimmer for providing viruses and plasmids.

This work was supported by Public Health Service grant AI-20017 from the National Institute of Allergy and Infectious Diseases.

REFERENCES

1. **Colston, E., and V. Racaniello.** 1995. Poliovirus variants selected on mutant receptor-expressing cells identify capsid residues that expand receptor recognition. J. Virol. **69:**4823–4829.
2. **Colston, E. M., and V. R. Racaniello.** 1994. Soluble receptor-resistant poliovirus mutants identify surface and internal capsid residues that control interaction with the cell receptor. EMBO J. **13:**5855–5862.
3. **Couderc, T., N. Guedo, V. Calvez, I. Pelletier, J. Hogle, F. Colbere-Garapin, and B. Blondel.** 1994. Substitutions in the capsids of poliovirus mutants selected in human neuroblastoma cells confer on the Mahoney type 1 strain a neurovirulent phenotype in mice. J. Virol. **68:**8386–8391.
4. **Couderc, T., A. Martin, C. Wychowski, M. Girard, F. Horaud, and R. Crainic.** 1991. Analysis of neutralization-escape mutants selected from a mouse virulent type 1/type 2 chimeric poliovirus: identification of a type 1 poliovirus with antigenic site 1 deleted. J. Gen. Virol. **72:**973–977.
5. **Filman, D. J., R. Syed, M. Chow, A. J. Macadam, P. D. Minor, and J. M. Hogle.** 1989. Structural factors that control conformational transitions and serotype specificity in type 3 poliovirus. EMBO J. **8:**1567–1579.
6. **Higuchi, R.** 1990. Recombinant PCR, p. 177–183. *In* M. Innis, D. Gelfand, J. Sninsky, and T. White (ed.), PCR protocols: a guide to methods and applications. Academic Press, Inc., San Diego, Calif.
7. **Hogle, J.** 1997. Personal communication.
8. **Hogle, J. M., M. Chow, and D. J. Filman.** 1985. Three-dimensional structure of poliovirus at 2.9 Å resolution. Science **229:**1358–1365.
9. **La Monica, N., W. Kupsky, and V. R. Racaniello.** 1987. Reduced mouse neurovirulence of poliovirus type 2 Lansing antigenic variants selected with monoclonal antibodies. Virology **161:**429–437.
10. **Liao, S., and V. Racaniello.** 1997. Unpublished data.
11. **Martin, A., C. Wychowski, T. Couderc, R. Crainic, J. Hogle, and M. Girard.** 1988. Engineering a poliovirus type 2 antigenic site on a type 1 capsid results in a chimaeric virus which is neurovirulent for mice. EMBO J. **7:**2839–2847.
12. **Mendelsohn, C., E. Wimmer, and V. R. Racaniello.** 1989. Cellular receptor for poliovirus: molecular cloning, nucleotide sequence and expression of a new member of the immunoglobulin superfamily. Cell **56:**855–865.
13. **Morrison, M. E., Y.-J. He, M. W. Wien, J. M. Hogle, and V. R. Racaniello.** 1994. Homolog-scanning mutagenesis reveals poliovirus residues important for virus binding and replication. J. Virol. **68:**2578–2588.

14. **Moss, E. G., and V. R. Racaniello.** 1991. Host range determinants located on the interior of the poliovirus capsid. EMBO J. **5:**1067–1074.
15. **Mosser, A., J. Sgro, and R. Rueckert.** 1994. Distribution of drug resistance mutations in type 3 poliovirus identifies three regions involved in uncoating functions. J. Virol. **68:**8193–8201.
16. **Mosser, A. G., and R. R. Rueckert.** 1993. WIN 51711-dependent mutants of poliovirus type 3: evidence that virions decay after release from cells unless drug is present. J. Virol. **67:**1246–1254.
17. **Murray, M. G., J. Bradley, X. F. Yang, E. Wimmer, E. G. Moss, and V. R. Racaniello.** 1988. Poliovirus host range is determined by a short amino acid sequence in neutralization antigenic site I. Science **241:**213–215.
18. **Palmenberg, A. C.** 1989. Sequence alignments of picornaviral capsid proteins, p. 211–241. *In* B. L. Semler and E. Ehrenfeld (ed.), Molecular aspects of picornavirus infection and detection. American Society for Microbiology, Washington, D.C.
19. **Racaniello, V. R.** 1995. Early events in infection: receptor binding and cell entry, p. 73–93. *In* H. A. Rotbart (ed.), Human enterovirus infections. ASM Press, Washington, D.C.
20. **Racaniello, V. R., and D. Baltimore.** 1981. Cloned poliovirus complementary DNA is infectious in mammalian cells. Science **214:**916–919.
21. **Racaniello, V. R., and D. Baltimore.** 1981. Molecular cloning of poliovirus cDNA and determination of the complete nucleotide sequence of the viral genome. Proc. Natl. Acad. Sci. USA **78:**4887–4891.
22. **Sanger, F., S. Nicklen, and A. R. Coulson.** 1977. DNA sequencing with chain-terminating inhibitors. Proc. Natl. Acad. Sci. USA **74:**5463–5467.
23. **Wien, M., S. Curry, V. Racaniello, D. Filman, and J. Hogle.** Interactions between poliovirus and its receptor: structural studies of poliovirus mutants that overcome receptor defects. Nat. Struct. Biol., in press.
24. **Yeates, T. O., D. H. Jacobson, A. Martin, C. Wychowski, M. Girard, D. J. Filman, and J. M. Hogle.** 1991. Three-dimensional structure of a mouse-adapted type2/type 1 poliovirus chimera. EMBO J. **10:**2331–2341.